Pharm Res (2012) 29:2225–2235
DOI 10.1007/s11095-012-0751-3

RESEARCH PAPER

High Concentration Formulation Studies of an IgG2 Antibody Using Small Angle X-ray Scattering

Charlotte Rode Mosbæk • Petr V. Konarev • Dmitri I. Svergun • Christian Rischel • Bente Vestergaard

Received: 7 February 2012 / Accepted: 27 March 2012 / Published online: 3 April 2012

ABSTRACT

Purpose Concentrated protein formulations are strongly influenced by protein-protein interactions. These can be probed at low protein concentration by e.g. virial coefficients. It was recently suggested that interactions are attractive at short distances and repulsive at longer distances. Measurements at low concentrations mainly sample longer distances, hence may not predict high concentration behavior. Here we demonstrate that small angle X-ray scattering (SAXS) measurements simultaneously collect information on interactions at short and long distances.

Methods IgG2 antibody samples at concentrations up to 122 mg/ml are analyzed using SAXS and compared to Circular Dichroism (CD), Fluorescence, Size Exclusion Chromatography (SEC) and Dynamic Light Scattering (DLS) analysis.

Results DLS and SEC analyses reveal attraction between antibodies at high concentrations. SAXS data analysis provides an elaborate understanding and shows both attractive and repulsive forces. The protein-protein interactions are strongly affected by excipients. No change in the solution state of IgG2 is observed at pH 4–8, while samples at pH 3 exhibit heavy oligomerization. The solution conformation of the examined IgG2 derived from SAXS data is a T-shape.

Conclusion SAXS analysis resolves simultaneous attractive and repulsive interactions, and details the effect of excipients on the interactions, while providing three-dimensional structural information from low-concentration samples.

C. R. Mosbæk • B. Vestergaard (✉)
Department of Drug Design and Pharmacology
University of Copenhagen
Copenhagen, Denmark
e-mail: bv@farma.ku.dk

C. R. Mosbæk • C. Rischel
Novo Nordisk A/S
Måløv, Denmark

P. V. Konarev • D. I. Svergun
European Molecular Biology Laboratory, Hamburg Outstation
Hamburg, Germany

KEY WORDS antibody · IgG2 · protein formulation · small angle x-ray scattering (SAXS) · solution characterization

ABBREVIATIONS

+NaCl	154 mM sodium chloride
+Sucrose	270 mM sucrose
A_2	second virial coefficient
BSA	bovine serum albumine
Buffer only	no further excipients
CD	circular dichroism
DLS	dynamic light scattering
D_{max}	maximal dimension
FF	form factor
K_D	diffusion virial coefficient
MM	molecular mass MM
P(r)	pair distance distribution function
R_g	radius of gyration
R_h	hydrodynamic radius
SAXS	small angle x-ray scattering
SEC	size exclusion chromatography
SF	the structure factor
SF_{eff}	effective structure factor
SLS	static light scattering

INTRODUCTION

Therapeutic antibodies are often administered at extremely high concentrations (>100 mg/ml). This is necessary to obtain the required biological effect and the acquired effective response, while avoiding a large dose volume (1) and is especially important for subcutaneous delivery (2).

In dilute protein solutions there are large inter-molecule distances. When protein concentration is increased the frequency of molecular collisions grows while the inter-molecule distances are reduced, increasing the importance of specific and unspecific interaction between individual protomers. It

was recently pointed out by Chari *et al.* (3) that interactions are predominantly attractive at short distances and repulsive at longer distances. At high concentration the protein solution behavior may be affected by formation of oligomers, either via reversible association or irreversible aggregation. Such interactions potentially influence protein activity or product safety (1,4), which makes an improved understanding of high concentration protein solute properties so important.

When designing protein formulations solution behavior must be monitored. However, biophysical characterization under accelerated stability studies may not be predictive for long term stability. This is a general challenge in formulation analysis of protein pharmaceuticals. For formulations at high protein concentrations (more than 10 % volume occupied by solute), protein-protein interactions are expected to be particularly important. With the methods at hand it is particularly difficult to adequately monitor solution behavior for high-concentration protein samples without lowering the protein concentration, i.e. not using the actual formulation state (3,5). Some techniques frequently used for studies of protein-protein interactions are Dynamic Light Scattering (DLS), Static Light Scattering (SLS) and Size Exclusion Chromatography (SEC), and SEC in particular involves significant dilution of the sample during analysis. Fluorescence and Circular Dichroism (CD) may be used as a control of folding stability, while CD is applied only at low to medium protein concentrations. For all these techniques the observed properties are difficult to relate to specific protein 3D-structural states and in particular, quantitative descriptions of distances/real-space interactions lack.

Small Angle X-ray Scattering (SAXS) data enable determination of physiologically and formulation relevant structural states of proteins in solution. The Intensity (I) of the x-rays scattered by the protein solution is detected as a function of the scattering angle. For scattering from a dilute solution, the scattering is a result of the intra-particle distances resulting in the form factor (FF) of a single particle. The scattering can be converted to real space correlations, represented by a pair distance distribution function (P(r)) and molecular mass (MM), radius of gyration (R_g), the maximal dimension (D_{max}) and *ab initio* models from the particle can be derived from the data (6).

For high concentration samples the interpretation of the scattering must be modified to take protein-protein interactions into account (6,7). The intensity, I(s), can then be described as the product of the particle scattering (FF) and a term describing the particle interactions (the structure factor (SF)):

$$I(s) \sim FF \times SF \quad (1)$$

For dilute solutions, where no protein-protein interactions are observed, the intensity equals FF, while for high concentration samples SF deviates from one, indicating attraction (larger than one) or repulsion (smaller than one) between the scatterers. This provides knowledge about the type and magnitude of interactions in highly concentrated protein samples.

SAXS is becoming increasingly accessible as a screening method. Sample size is shrinking (10–100 µl sample volumes are routinely applied at several beam-lines) and robotics and micro fluidics are being developed along with remote operation of synchrotron beam-line experiments (8,9). This may make SAXS a valuable technique when designing protein formulations in the future.

MATERIALS AND METHODS

Sample Preparation

The human anti-EGFR IgG2 antibody, panitumumab (Vectibix© produced by Amgen) is used as a model antibody. Panitumumab is a 147 kDa antibody formulated at 20 mg/ml in a sodium acetate tri hydrate, 150 mM sodium chlorid solution at pH 5.8. In this study, three buffer compositions were chosen for investigation. Buffers contain 10 mM citrate at pH 5.8 with addition of either 154 mM sodium chloride (in the following called +NaCl), 270 mM sucrose (in the following called +Sucrose) or no further excipients (in the following called Buffer only), respectively. Furthermore, +NaCl samples were produced at pH 3, 4, 5, 5.8, 7 and 8, using a 10 mM potassium phosphate buffer instead of citrate for pH 7 and 8. Samples were dialyzed 24 h against the respective buffers and stored at 4 °C. The dialysis buffers were used for background measurements. Samples measured at concentrations higher than 12 mg/ml were concentrated using Amicon® Ultra centrifugal filters from Millipore (MWCO 30.000). The protein concentration was determined in relation to the starting product (20 mg/ml) using UV absorbance at 280 nm when the protein concentration was adequately low. For high protein concentration solutions, a slightly different approach was used. At high concentrations there is no longer a linear concentration dependency at 280 nm, hence the ratio between absorbance at 280 nm and 297 nm was determined a low protein concentration, and this ratio was used to calculate the concentration from measurements at 297 nm. +NaCl, +Sucrose and Buffer only samples at pH 5.8 were produced in the concentration range 1.5–119 mg/ml, while +NaCl samples at pH 3–5 and 7–8 were produced at 1.5–10 mg/ml. Immediately before data acquisition all samples were centrifuged 10 min at 13000 rpm at 4 °C. A redilution (re) test was performed by dilution of the most concentrated +NaCl, Buffer only and +Sucrose samples to approximately 3 mg/ml.

Samples were stored for a maximum of 24 h at a temperature of 4 °C prior to data acquisition.

SAXS: Basic Data Evaluation

SAXS data were collected on all samples using synchrotron radiation following standard procedures at beamline X33 at the European Molecular Biology Laboratory on the DORIS III storage ring (DESY, Hamburg, Germany). A momentum transfer range of 0.07–5.0 nm^{-1} ($s=4\pi\sin(\theta)/\lambda$, 2θ is the scattering angle and λ is the x-ray wavelength ($\lambda=1.5$ Å)) was covered. Data collection was carried out during two separate data collections both covering exposure times of 2 min at 8 °C, while using a MAR345 image plate and a PILATUS 1 M pixel X-ray detector, respectively. The exposure time at the second data collection was divided into four separate exposures of 30 s each, and individual frames were compared for evaluation of potential x-ray induced damage. Data from undamaged protein were averaged to give the final data file. The data were normalized to the intensity of the incident beam and corrected for the respective detector response. Data analysis was performed using the software suite ATSAS (10,11). R_g was evaluated by the Guinier approximation (using the s range satisfying the criteria: $s*R_g<1.3$) and the MM was estimated from the extrapolated forward scattering intensity (I(0)) using a reference solution of Bovine Serum Albumin (BSA) (5.7 mg/ml, 50 mM HEPES pH 7.4) as molecular mass (MM) reference. The P(r) were evaluated using GNOM (12,13) yielding also D_{max} within the scatterer. The effective structure factor (SF_{eff}) contribution was determined by division of the total intensity by the individual FF. The FF was found by merging low concentration data, where no protein-protein interactions were observed, with higher concentration data in areas where the scattering patterns were identical for all concentrations. Before division the noise at low scattering angles in the FF originating from the low concentration samples was reduced manually by comparison to the curve fit obtained from GNOM. Theoretical scattering curves from high resolution crystal structures were calculated using the program Crysol (14).

SAXS-Based *Ab Initio* Modelling

Ab initio structures were obtained using the program Dammif (15). A simulated annealing protocol is used to build a compact bead model of uniform scattering length density, while minimizing the discrepancy between the experimental and calculated curves at low resolution (in this work scattering angles up to 2.9 nm^{-1} are used). Ten individual models were spatially superposed and the normalized spatial discrepancy (NSD-values) evaluated before similar models were averaged (as is standard procedure in the program suite Damaver (16)). The resulting averaged and unfiltered model was used as a starting search volume (input volume in Dammif) and ten refined models were built and averaged in Damaver. The final averaged model was calculated restricted to a volume corresponding to the typical excluded volume of the ten initial models.

Fluorescence

Fluorescence measurements were performed on a Varian Cary Eclipse fluorescence spectrophotometer at 20 °C. The tryptophan fluorescence was monitored between 310 and 450 nm, with an excitation wavelength of 300 nm. The spectra were recorded with a scan rate of 120 nm/min. The excitation and emission slits were set to 5 nm and 2.5 nm, respectively. 5 scans were carried out for each sample to improve statistics. Data were collected at pH 5.8 in +NaCl, Buffer only and +Sucrose at protein concentrations from 2.9 to 122 mg/ml and in +NaCl at pH 3–8 at 3 and 10 mg/ml. All data were normalized at the maximum intensity.

CD

CD measurements were carried out using a Chirascan CD Spectrophotometer. The studies were performed in a 0.1 mm path length cell at a scan rate of 40 nm/min from 195 to 310 nm. Data were collected at pH 5.8 in +NaCl, +Sucrose and Buffer only and in +NaCl at pH 3–5 and 7–8 all at 3 mg/ml protein concentration and the buffer signal was subtracted.

SEC-SLS

Samples were analyzed using an Agilent 1100/1200 Chemstation HPLC system with a BioSep3000 SEC column connected to a miniDAWN (Wyatt Technology) and a differential refractometer. 120 µg protein in a volume range of 1–30 µl were loaded from each sample of concentration 3–119 mg/ml at 4 °C. PBS buffer at pH 7.4 was used as the mobile phase for all samples at a rate of 0.32 ml/min. The measured 90° light scattering signal and refractive index was used for MM determination using a reference solution of BSA (data not shown). The UV absorbance at 280 nm was used to monitor the protein elution from the SEC column. The dimer content was calculated from the area under the peak. All data were normalized for the monomer peak intensity.

DLS

DLS was measured on a DynaPro Titan instrument from Wyatt Technology with a laser wavelength of 832.5 nm.

The measurements were carried out in 1.5 mm path length cuvettes at 20 °C, where 40 acquisitions of 5 s each were collected with auto adjustment of laser power.

Data were collected at pH 5.8 in +NaCl, +Sucrose and Buffer only at protein concentrations from 2.9 to 122 mg/ml and in +NaCl at pH 3–5 and 7–8 at 3 and 10 mg/ml. Furthermore the intensity was measured with changing laser power (2–28 %) for one +NaCl pH 5.8 sample at 10 mg/ml and used for normalization of the intensity to a laser power corresponding to 1 %. The hydrodynamic radius (R_h) for +Sucrose samples was normalized for difference in viscosity.

The second virial coefficient (A_2) was calculated from the plot of C/I *vs.* C, using the following formula (17,18):

$$\frac{C}{I} = \frac{1}{MM \times K_1} + \left(\frac{2 \times A_2 \times C}{K_1}\right)$$

where C is the concentration, I the intensity, and K_1 a constant defined as $(K \times I_l \times V)/r^2$, I_l the laser intensity, V the exposed sample volume, r the distance from the sample to the detector and K is defined as

$$4\pi^2 n_0^2 \frac{\left(\frac{dn}{dC}\right)^2}{N_A \lambda_0^4}$$

with n_0 as the solvent refractive index, N_A Advogadro's number and λ_0 the wavelength of the laser in vacuum. For high concentration samples a higher degree polynomial can be included in the calculation of A_2.

The diffusion virial coefficient (K_D) was calculated from the plot of $1/R_h$ *vs.* C, using the following formula:

$$\frac{1}{R_h} = \frac{1}{R_{h(0)}} + K_D \times \frac{C}{R_{h(0)}}$$

Where R_h is the hydrodynamic radius and $R_h(0)$ the radius of gyration at infinite dilution.

RESULTS

Fluorescence

The fluorescence spectra of +NaCl pH 5.8 at 3–119 mg/ml are shown in Fig. 1a. All samples exhibit the same fluorescence spectra regardless of concentration, indicating no detectable change in tryptophan side chain packing between proteins at high and low concentration. Identical spectra were observed for Buffer only and +Sucrose samples (data not shown). Figure 1b shows the fluorescence spectra at 3 mg/ml at varying pH and buffer composition. The spectra are identical, except for samples at pH 3, where the fluorescence peak is shifted against higher wavelengths, indicating solvent exposure of tryptophan side chains, probably due to partial unfolding of the protein.

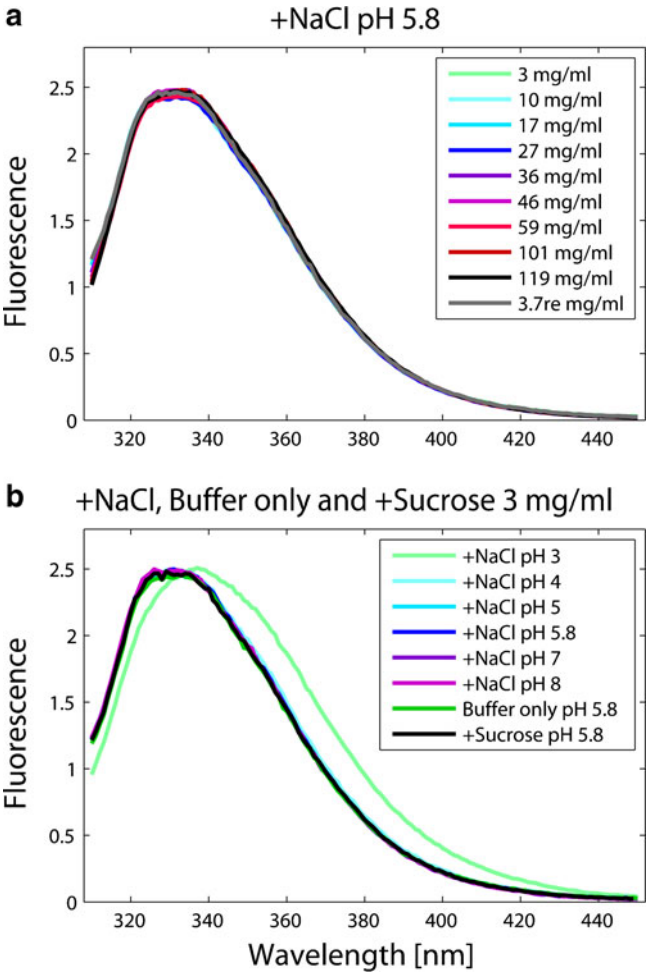

Fig. 1 (**a**) Fluorescence spectra for +NaCl pH 5.8 samples in the concentration range 3–119 mg/ml. 3.7re indicates a sample rediluted from 119 mg/ml. (**b**) Fluorescence spectra for +NaCl samples in the pH range 3–8 and Buffer only and +Sucrose samples at pH 5.8 all at 3 mg/ml. Data at 10 mg/ml show the same pattern (data not shown).

Circular Dichroism

The CD spectra for +NaCl, Buffer only and +Sucrose at 3 mg/ml are shown in Fig. 2. The spectra are identical for all three buffers and for +NaCl at pH 4–8. The spectra exhibit a minimum at 218 nm, indicating a composition of primarily β-sheet structure, as is typical for an immunoglobulin antibody. +NaCl pH 3 deviates from the other samples by a stronger negative signal at 200–230 nm. Hence, no changes in secondary structure are observed for the investigated buffer compositions at a concentration of 3 mg/ml, except when pH is decreased to pH 3.

SEC-SLS

The UV absorbance at 280 nm from the SEC column elutions have been compared for varying buffer composition and antibody concentrations, see Fig. 3a and b. A monomer and a dimer peak are seen for all samples, and are verified

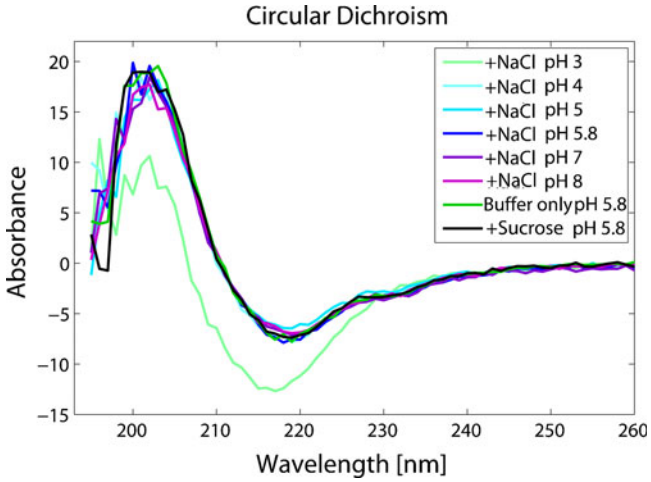

Fig. 2 CD spectra from +NaCl samples in the pH range 3–8 and Buffer only and +Sucrose samples at pH 5.8 all at 3 mg/ml.

by light scattering and refractive index measurements (data not shown). The dimer peak (see Fig. 3a for +NaCl data), grows as the protein concentration is increased. The increase in dimer content is observed in all three buffers at pH 5.8 at an identical rate (see Fig. 3b), hence the method does not distinguish between +NaCl, +Sucrose and Buffer only samples (when using PBS as the mobile phase). The increased dimer content indicates an increase in protein-protein interactions at higher concentrations.

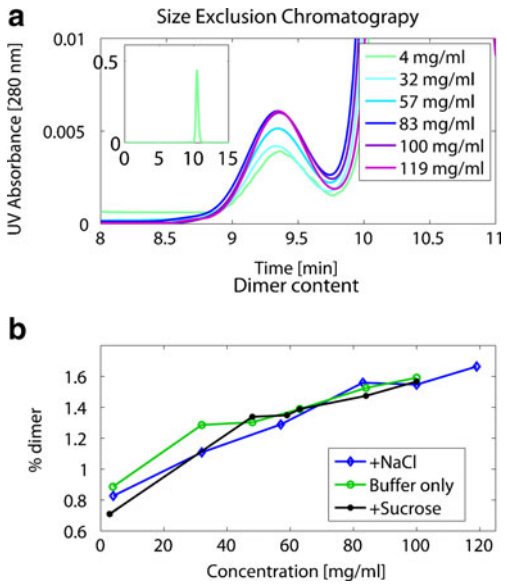

Fig. 3 (**a**) Chromatogram showing the elution from the SEC column of +NaCl pH 5.8 samples at a concentration range of 4–119 mg/ml. Upper left corner shows the elution from 0 to 15 min for the 4 mg/ml sample, while the background depicts a zoom-in on the elution profile of the dimer peak for all concentrations. (**b**) The calculated dimer content as a function of concentration.

DLS

R_h was determined for all samples (see Fig. 4b), and the value increases at increasing concentration. Buffer only has the steepest increase in R_h values, while +Sucrose and +NaCl samples develop comparably at the investigated experimental conditions. R_h values for +NaCl 3 and 10 mg/ml pH 3–8 are shown on Fig. 4a. pH 3 deviates

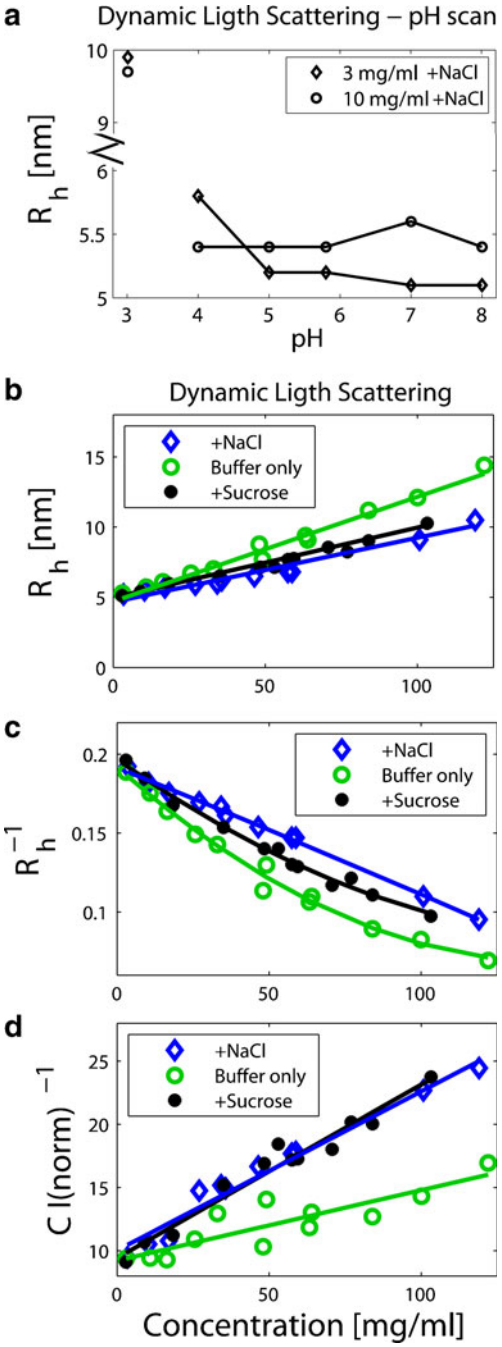

Fig. 4 (**a**) R_h shown as a function of pH for +NaCl samples at 3 and 10 mg/ml. (**b**, **c** and **d**) R_h, $C * I^{-1}$ and R^{-1}, respectively, shown as a function of concentration for +NaCl, Buffer only and +Sucrose samples. The lines are results of first and secondary order polynomial fits.

Table I The Calculated Second Virial Coefficient (A_2) and the Diffusion Virial Coefficient (K_D)

Sample	A_2 (mol ml/g^2)	K_D (ml/g)
+NaCl	$4.42 * 10^{-5}$	$-4.18 * 10^{-3}$
Buffer only	$2.06 * 10^{-5}$	$-8.86* 10^{-3}$
+Sucrose	$4.96 * 10^{-5}$	$-7.2* 10^{-3}$

significantly indicating oligomerization at low pH. The second virial coefficient and the diffusion virial coefficient (see Table I), were calculated from the plot of C/I *vs.* C and $1/R_h$ *vs.* C (see Fig. 4c and d, respectively). A_2 values are positive, while K_D values are negative.

SAXS

Solution Structure of Panitumumab

SAXS data were collected from samples in the concentration range 1.5–122 mg/ml. The FF's for the three buffer types were identical, see Fig. 5. This suggests that the protein solution behavior is similar at low concentrations under the three buffer conditions evaluated in this study. The observed molecular masses, (155 kDa), correspond to that of a monomer solution and R_g and D_{max} for the FF were determined to be 5.1 nm and 16.4 nm respectively.

The FF's were compared to the theoretical scattering calculated from antibody x-ray crystal structures, see Fig. 6a (pdb entries: 1HZH (IgG B12 human), 1IGY (IgG1 mouse) and 1IGT (IgG2A mouse)). None of the theoretical scattering curves calculated from the x-ray crystal structures result in a good fit to the experimental data, but the real space representation P(r) for 1IGY (see Fig. 6b) reveals an overall shape with pronounced similarities to the P(r) calculated from the experimental data. This crystal structure deviates from the other antibody x-ray crystal structures by having a more pronounced bend in the hinge region placing the Fc fragment almost perpendicular to the plane formed by the Fab domains.

If assuming that no pronounced structural heterogeneity resides in the solute, *Ab initio* modeling results in a low resolution solution model of the scattering particle. Modeling was carried out using the P(r) function derived from the FF of +NaCl and the resulting model and corresponding fit to the experimental data is shown on Fig. 7. The *ab initio* model is compared to the x-ray crystal structure 1IGY. In

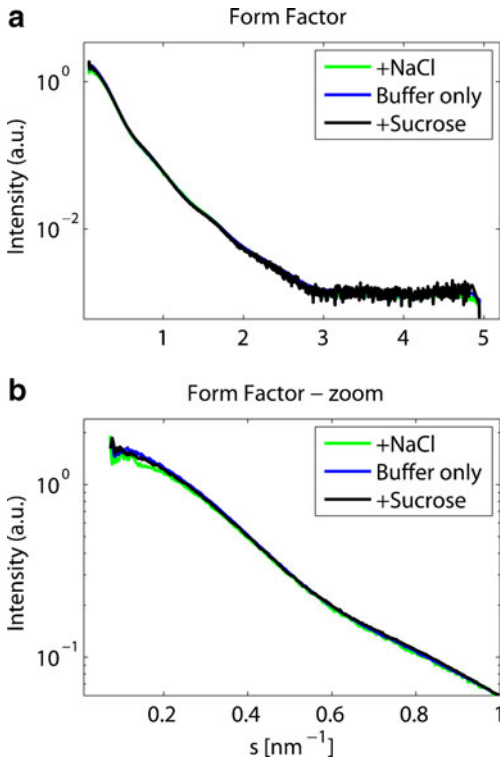

Fig. 5 (**a**) SAXS data curves representing the form factor of +NaCl, Buffer only and +Sucrose at 3 mg/ml. The curves are scaled between 0.75 nm^{-1} and 1.7 nm^{-1}. The three samples exhibit highly similar scattering patterns (**b**) zoom of A.

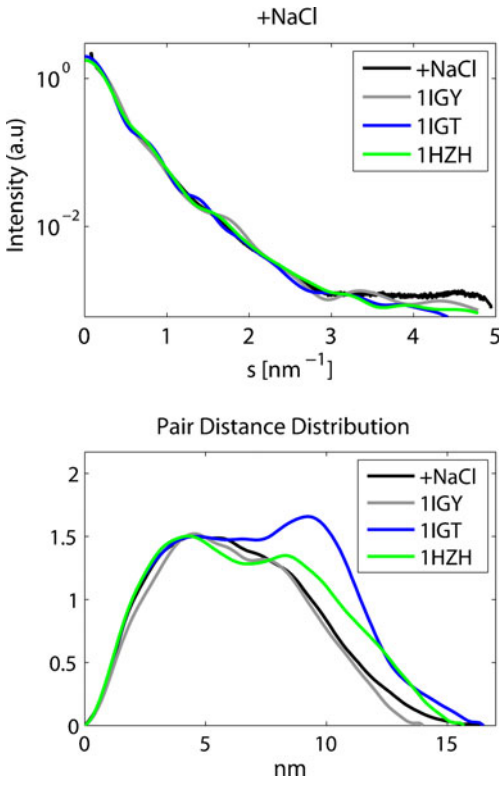

Fig. 6 (**a**) Theoretical scattering curves of antibody X-ray crystal structures (pdb entries 1HZH, 1IGT and 1IGY) and fit to the FF of the +NaCl sample. (**b**) Pair distance distribution function of the theoretical scattering curves and the FF of +NaCl (normalized at 4.5 nm).

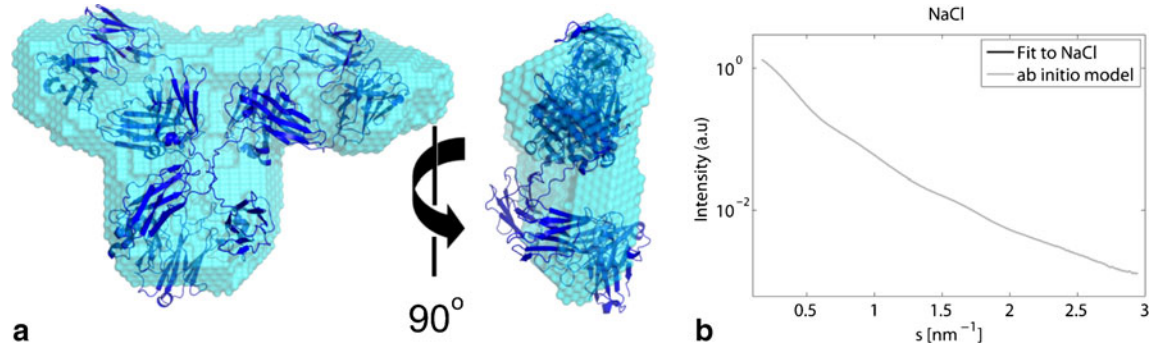

Fig. 7 (**a**) Front and side view of the *ab initio* model of Panitumumab and superposition of 1IGY (produced in Pymol (20)). (**b**) Fit between the calculated scattering curve from the model and the experimental data.

the represented orientation, the upper part of the *ab initio* model is assumed to span the Fab fragments. The model shows an overall T-shape with a tip to tip Fab fragment distance of 16.4 nm. The angle between Fab arms is increased from what is observed in the crystal structure (1IGY). The Fc fragment is bent towards one of the Fab arms. A side view of the model shows the thickness of the molecule to be approximately 2.5 nm, which indicates that all domains are oriented in approximately the same plane. A minor twist is observed within the part of the model corresponding to the end of the Fab arm placed opposite to the Fc domain.

High Concentration Solution Behaviour

As is seen in Fig. 8, when concentration is increased the scattering deviates from the FF at low scattering angles (below 1 nm^{-1}), while the remaining part of the scattering curve is not affected. This deviation is caused by the SF, which is a result of protein-protein interactions. The concentration series from the three investigated buffer compositions exhibit different concentration dependency.

To further explore the concentration mediated interactions between proteins the SF_{eff} was isolated, by division of the scattering curves by the FF. The SF_{eff} is a result of attraction and repulsion between molecules combined with excluded volume effects and is shown on Fig. 9. Increased repulsion between molecules will decrease the magnitude of the SF_{eff}, while increased attraction will increase the SF_{eff}. The SF_{eff} clearly shows that both repulsion and attraction between molecules occurs when the antibody is concentrated. In the +NaCl sample repulsion between molecules dominates and becomes more pronounced at higher concentration. Repulsion is mainly observed in the +Sucrose samples until 38 mg/ml is reached. When the concentration is further increased attraction also becomes significant. The Buffer only samples are affected by both repulsion and attraction between molecules at protein concentration from 33 mg/ml and above while attraction between scatterers becomes remarkable when the antibody is concentrated above 80 mg/ml. Figure 9b, d and e compares the SF_{eff} of +NaCl, Buffer only and +Sucrose at approximately 35, 60 and 120 mg/ml. The SF_{eff} very clearly shows that the interactions between molecules depend on buffer composition. Distinctly increased attraction/oligomerization is observed in the Buffer only sample along with significant repulsive effects. Repulsion dominates the +NaCl and the +Sucrose samples while attractive forces are also observed particularly in the +Sucrose sample. In general, attraction and repulsion is observed when concentration is increased and repulsion is evident from scattering angles of 0.6 nm^{-1} corresponding to real space center-to-center distances of approximately 10.5 nm.

A redilution test was performed to test for permanent effects on the protein solution conformation caused by the crowded environment in highly concentrated samples (see Fig. 10). The shape of the scattering curve is restored for all buffer types only revealing a minor increase in intensity for rediluted samples at scattering angles below 0.6 nm^{-1}, hence illustrating recovery of the solution state of the antibody.

pH and Batch Variations

The influence of pH on the antibody conformation was investigated in +NaCl buffer at 3 mg/ml. Figure 11 shows data curves from antibodies in +NaCl buffer at pH 3, 4, 5, 6, 7 and 8. Only pH 3 deviates from the other data curves and exhibits a distinctly different scattering pattern indicating heavy oligomerization. pH variation between 4 and 8 does not influence the solution conformation of the antibody.

SAXS data from Panitumumab from two different batches dialyzed into +NaCl pH 5.8 buffer using identical procedures is shown on Fig. 12. The SAXS data analysis detects a small variation between the two samples, while identical R_h values of 5.2 nm were observed

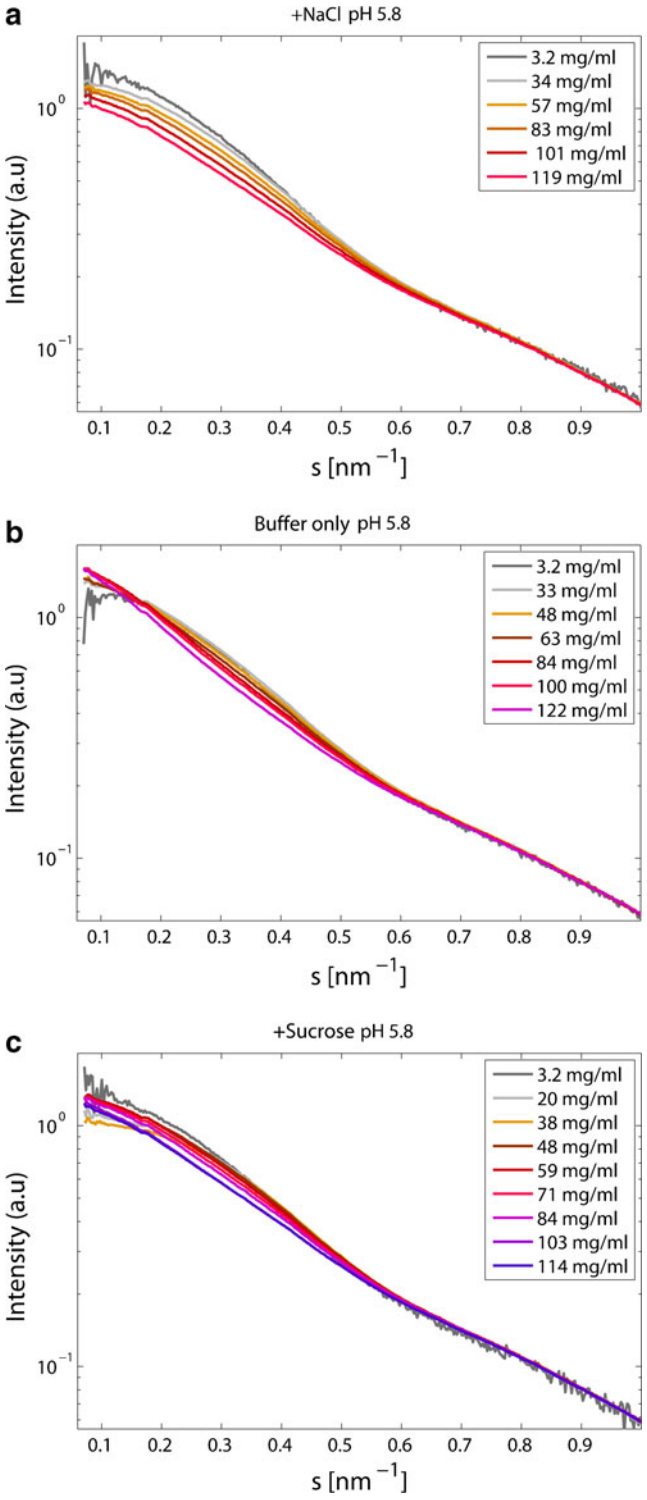

Fig. 8 Scattering curves of (**a**) +NaCl, (**b**) Buffer only and (**c**) +Sucrose at scattering angles below 1 nm^{-1}, where concentration dependence is observed. The curves are scaled at 0.75–1.7 nm^{-1}.

from DLS analysis. This illustrates the high sensitivity of the SAXS technique, to detect minor changes in solution behavior.

DISCUSSION

A comprehensive analysis of the solution conformation of Panitumumab has been conducted. The solution structure of Panitumumab is seemingly identical at low concentrations while applying three different excipients and over a variety of pH values. This suggests that there is little or no structural heterogeneity in the samples investigated. The antibody has a bent T-shape conformation in solution when no interaction between molecules is observed. The tip of the Fab arms are separated by 16.4 nm and the angle between Fab arms is increased from what is observed for 1IGY in order to obtain an overall T-shape, even more pronounced than in the x-ray crystal structures. The thickness of the molecule is approximate 2.5 nm, which indicates that all domains are oriented in the same plane. None of the techniques used in the study show changes in solution behavior at concentrations below 3 mg/ml when changing buffer composition or varying pH between 4 and 8. Only at pH 3 the samples show a distinctly different solution behavior indicating heavy oligomerization.

When increasing the protein concentration of the antibody solutions no change in fluorescence signal is detected, while CD cannot be performed at high protein concentration. SEC analysis reveals increasing formation of dimers when protein concentration is increased, which indicates attraction between monomers. Since the samples were concentrated less than 1 day before the analysis, the difference in dimer content is formed in a relatively rapid process, possibly a reversible equilibrium, although we have not explored this further in this work. The amount of dimer is accurately quantified, and the dimer content is the same for all three formulations within experimental error. This either suggests that the presence of sucrose or NaCl at the concentrations investigated have no influence on the average amount of dimer which is formed, or, alternatively, that a new equilibrium is rapidly reached after injection on the column. Hence, in this case the elution buffer (PBS) is more important than the buffer in the injected formulation. The positive A_2 values in Table I indicate attractive interactions between protein molecules, with similar interaction strengths in the NaCl and sucrose formulations and weaker attraction in the buffer only samples. K_D values are negative. This can in theory be due to either repulsive or attractive interactions (17,18), but experience with monoclonal antibodies suggest that a negative K_D value is indicative of attractive interactions (19). The K_D value indicates the largest attraction between molecules in buffer only, less in sucrose and least in NaCl; a different pattern than shown by the A_2 values. None of these methods are capable of detecting the simultaneous presence of attractive and repulsive interactions.

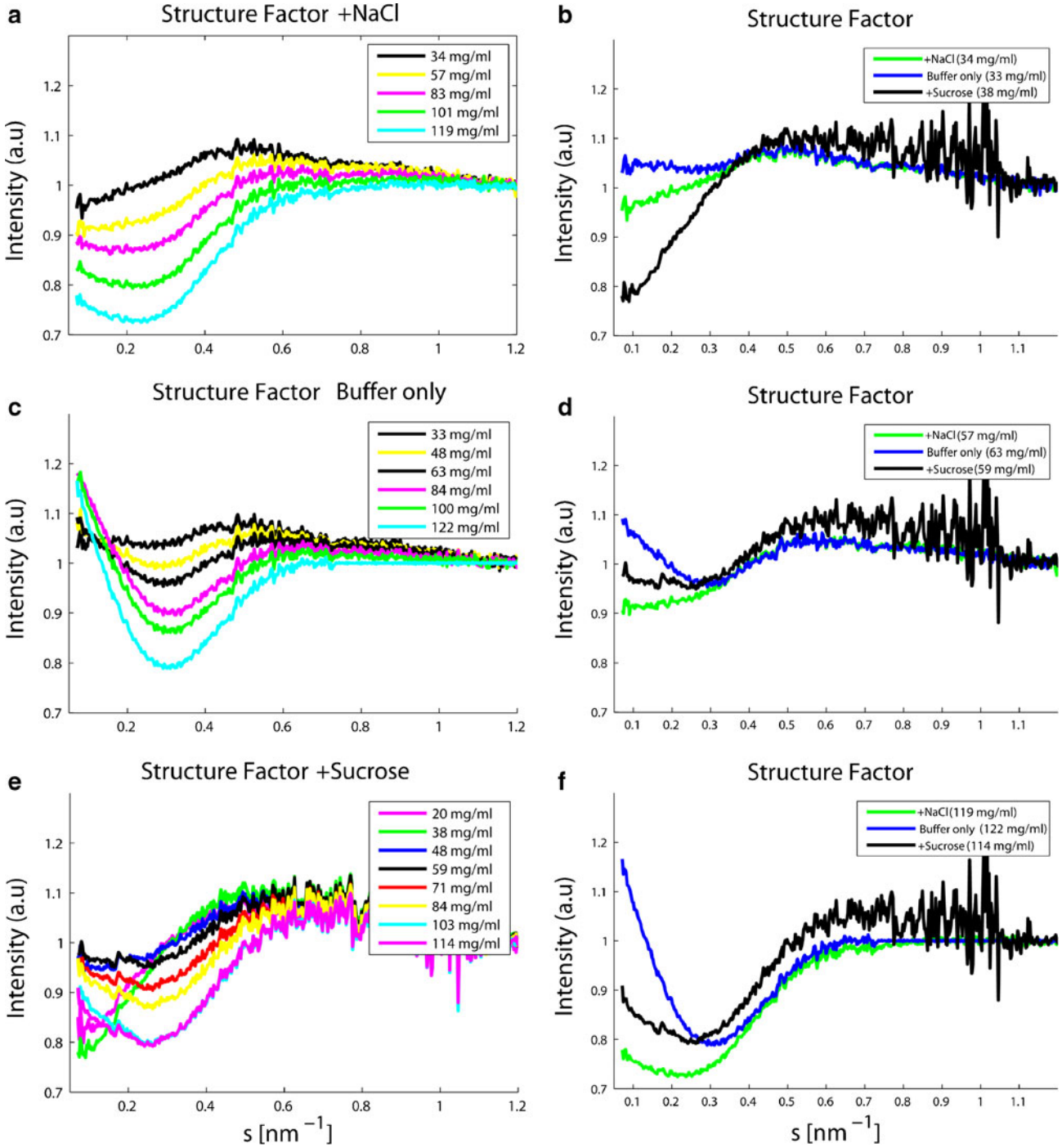

Fig. 9 SF_{eff} of (**a**) +NaCl, (**c**) Buffer only and (**e**) +Sucrose. (**b**, **d**, **e**) SF_{eff} of +NaCl, Buffer only and +Sucrose at approximately 35, 60 and 120 mg/ml, respectively.

The SAXS analysis, on the other hand, clearly reveals that both repulsive and attractive forces appear in high concentration samples. At low concentrations +NaCl and +Sucrose show mainly repulsive interactions, as also seen in the SLS data. The positive virial coefficient A_2 measured from SLS data for all three conditions indicate predominantly repulsive interactions. We also calculated virial coefficients from extrapolation of SAXS data to q=0. The results were much smaller than the results obtained by SLS, probably as a result of the larger scattering vectors included in SAXS data analysis, which comprises additional contributions from protein interactions (data not shown). At higher concentrations, the SAXS data show that repulsive forces are dominating in +NaCl samples, while both

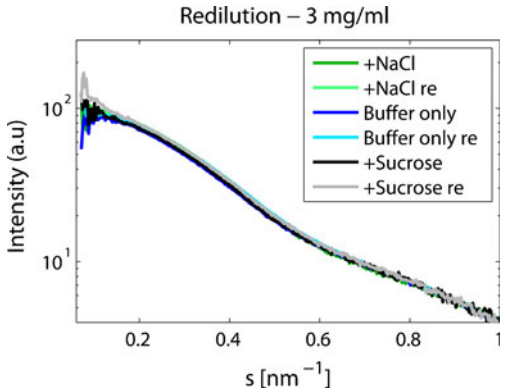

Fig. 10 Scattering curves of +NaCl, Buffer only and +Sucrose at scattering angles below 1 nm^{-1}. Re indicate a sample rediluted from the sample at highest concentration used in the study. The curves are scaled between 0.75 and 1.7 nm^{-1}.

attraction and repulsion is observed in +Sucrose and Buffer only samples. Different development rates of attraction and repulsion are observed for the three. Attractive interactions are much stronger in Buffer only samples than in +Sucrose and +NaCl, hence the excipients clearly stabilize the antibody solution and possibly prevent irreversible aggregation. In general, attraction and repulsion is observed when concentration is increased and repulsion is evident from distances of approximately 10.5 nm. SAXS data show that the solution conformation of all concentrated samples could be restored, hence the interaction process is reversible and the crowded environment did not induce permanent structural changes within the antibody. Furthermore, changes in batch variation between highly identical samples were observed emphasizing the high sensitivity of the technique.

The experimental differences between the techniques employed in the present study mean that direct comparison between the types of datasets to some extent is complicated.

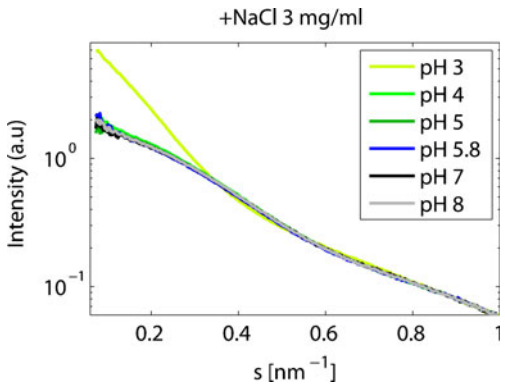

Fig. 11 Scattering curves of +NaCl pH 3–8 at scattering angles below 1 nm^{-1}. Only the scattering recorded at pH 3 deviates from the other scattering curves and indicates significant oligomerization.

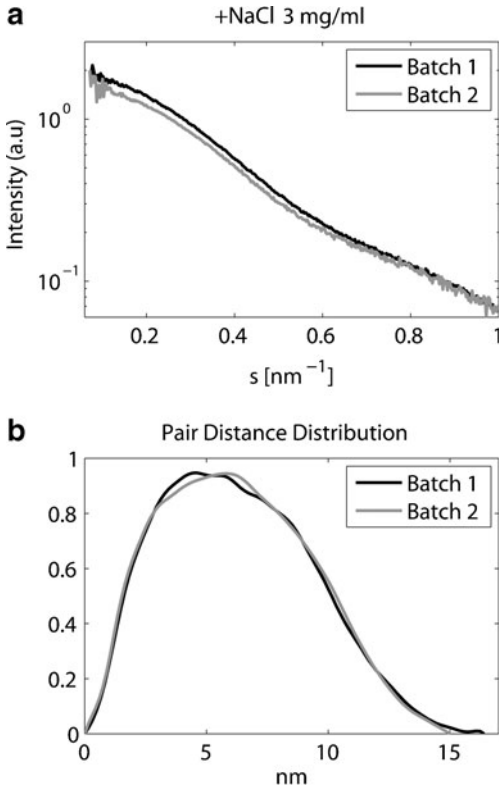

Fig. 12 (**a**) Scattering curves of +NaCl pH 5.8 originating from two separate batch preparations at scattering angles below 1 nm^{-1}. Both batches correspond to the same oligomerization state. The curves are scaled at 0.75–1.7 nm^{-1}. (**b**) Pair distance distribution function of Batch 1 and Batch 2 (normalized at 5 nm).

The wavelength applied in DLS means that very large particles (such as large-scale aggregates or contaminations of non-protein particles) greatly influence DLS data, while SAXS data are devoid of such disturbance. Both methods, however, do probe sizes in the range that is studied here, and there are no indications of the presence of very large-scale aggregates in our samples. We conclude that comparison between these types of data is useful.

CONCLUSION

This work shows that interaction between antibodies is highly dependent on buffer excipients. The protein-protein interactions occurring at high concentrations were investigated by SAXS data analysis and show that attractive and repulsive interactions exist simultaneously between antibodies, and also reveal the concentration dependent development of the two types of interaction. The three dimensional solution conformation of the IgG2 antibody under the experimental conditions examined reveals a T-shaped conformation with a Fab fragment tip-to-tip distance of 16.4 nm with all domains oriented in the same plane.

ACKNOWLEDGMENTS & DISCLOSURES

This work was financially supported by Novo Nordisk A/S, the Drug Research Academy, The Danish Council for Independent Research | Medical Sciences and DANSCATT.

REFERENCES

1. Wang W, Singh S, Zeng DL, King K, Nema S. Antibody structure, instability, and formulation. J Pharm Sci. 2007;96(1):1–26.
2. Shire SJ, Shahrokh Z, Liu J. Challenges in the development of high protein concentration formulations. J Pharm Sci. 2004;93(6): 1390–402.
3. Chari R, Jerath K, Badkar AV, Kalonia DS. Long- and shortrange electrostatic interactions affect the rheology of highly concentrated antibody solutions. Pharm Res. 2009;26(12):2607–18.
4. Yadav S, Liu J, Shire SJ, Kalonia DS. Specific interactions in high concentration antibody solutions resulting in high viscosity. J Pharm Sci. 2010;99:1152–68.
5. Saluja A, Badkar AV, Zeng DL, Nema S, Kalonia DS. Application of high-frequency rheology measurements for analyzing protein-protein interactions in high protein concentration solutions using a model monoclonal antibody (igg2). J Pharm Sci. 2006;95(9):1967–83.
6. Svergun DI, Koch MHJ. Small-angle scattering studies of biological macromolecules in solution. Rep Prog Phys. 2003;66:1735–82.
7. Hansen S. Simultaneous estimation of the form factor and structure factor for globular particles in small-angle scattering. J Appl Cryst. 2008;41:436–45.
8. Petoukhov MV, Konarev PV, Kikhney AG, Svergun DI. ATSAS 2.1 - towards automated and web-supported small-angle scattering data analysis. J Appl Cryst. 2007;40:223–8.
9. Toft KN, Vestergaard B, Nielsen SS, Snakenborg D, Jeppesen MG, Jacobsen JK, Arleth L, Kutter JP. High-throughput small angle x-ray scattering from proteins in solution using a microfluidic front-end. Anal Chem. 2008;80:3648–54.
10. Konarev PV, Volkov VV, Sokolova AV, Koch MHJ, Svergun DI. PRIMUS: a windows PC-based system for small-angle scattering data analysis. J Appl Cryst. 2003;36:1277–82.
11. Konarev PV, Petoukhov MV, Volkov VV, Svergun DI. ATSAS 2.1, a program package for small-angle scattering data analysis. J Appl Cryst. 2006;39:277–86.
12. Svergun DI, Semenyuk AV, Feigin LA. Small-angle-scattering-data treatment by the regularization method. Acta Crystallogr A Found Crystallogr. 1988;A44:244–50.
13. Svergun DI. Determination of the regularization parameter in indirect-transform methods using perceptual criteria. J Appl Cryst. 1992;25:495–503.
14. Svergun DI, Barberato C, Koch MHJ. Crysol-a program to evaluate X-ray solution scattering of biological macromolecules from atomic coordinates. J Appl Cryst. 1995;28:768–73.
15. Franke D, Svergun DI. DAMMIF, a program for rapid ab-initio shape determination in small-angle scattering. J Appl Cryst. 2009;42:342–6.
16. Volkov VV, Svergun DI. Uniqueness of ab initio shape determination in small angle scattering. J Appl Cryst. 2003;36:860–4.
17. Teraoka I. Polymer solutions: An introduction to physical properties, John Wilet & sons, Inc., 2002.
18. Cao A. Light Scattering. Recent Applications. Anal Lett. 2003; 36:3185–225.
19. Yadav S, Shire SJ, Kalonia DS. Viscosity behavior of high-concentration monoclonal antibody solutions: correlation with interaction parameter and electroviscous effects. J Pharm Sci. 2012;101:998–1011.
20. DeLano WL. The PyMOL molecular graphics system. Palo Alto: DeLano Scientific LLC; 2008.